TRADITIONAL AND INTEGRATIVE MEDICINE

Trad Integr Med, Volume 11, Issue 2, Spring 2026

Original Research

Kaempferol-Silver Nanoparticle Quercetin Gel for Psoriasis: An *In Vitro* and *In Vivo* Preclinical Study

Siddhi Fogueri, Mrityunjaya Patil*

Department of Pharmacognosy, KLE College of Pharmacy, JNMC Campus, Nehru Nagar, Belagavi-590010, Karnataka, India

Received: 3 Oct 2025 **Revised:** 12 Feb 2026 **Accepted:** 15 Feb 2026

Abstract

This study focuses on developing a novel topical silver nanoparticle (AgNPs) based gel for psoriasis, a chronic inflammatory skin disease affecting over 60 million people worldwide. Conventional therapies are limited by side effects and poor efficacy, highlighting the need for safer and more effective alternatives.Kaempferol (KMP), a natural flavonoid with anti-psoriatic activity, has poor solubility and low bioavailability. To overcome these limitations, kaempferol-silver nanoparticles (KSNPs) were synthesized and incorporated into a quercetin (QRT) gel.The efficacy of the KSNP-loaded QRT gel was assessed through *in vitro* studies in human keratinocytes, skin irritation testing, and *in vivo* evaluation in an imiquimod (IMQ)-induced psoriasis model. The formulation aims to enhance skin penetration, stability, and therapeutic outcomes, providing a promising strategy for improved psoriasis management. The formulation exhibited 89.54 ± 1.27% entrapment efficiency with 85.15% cumulative drug release over 24 hours. *In vitro* assays (HRBC membrane stabilization and protein denaturation inhibition) confirmed strong anti-inflammatory activity, while skin irritancy studies indicated reduced toxicity through KMP-mediated bio-reduction of silver nanoparticles. In the IMQ-induced psoriasis model, topical application of the gel marked a visible reduction in PASI scores, further supported by histopathological evidence. Overall, the KSNP-loaded QRT gel, combining the complementary effects of KMP and QRT, demonstrated controlled drug release and promising therapeutic efficacy for psoriasis and related inflammatory skin disorders.The KSNP-loaded QRT gel shows a promising, safe, and effective topical therapy for psoriasis, leveraging the anti-inflammatory effects of KMP and QRT with enhanced bioavailability through nanoparticle formulation

Keywords: Psoriasis; Anti-psoriatic activity; Metal nanoparticle; Carbopol 934; Gel; Silver nanoparticles; Kaempferol; Quercetin; Anti-inflammatory; Imiquimod model.

http://doi.org/10.18502/tim.v11i2.22053

Citation: Fogueri S, Patil M**. Kaempferol-Silver Nanoparticle Quercetin Gel for Psoriasis: An *In Vitro* and *In Vivo* Preclinical Study.** Trad Integr Med 2026;11(2):142-161. http://doi.org/10.18502/tim.v11i2.22053

*Corresponding Author:Mrityunjaya Patil
Department of Pharmacognosy, KLE College of Pharmacy, JNMC Campus, Nehru Nagar, Belagavi-590010, Karnataka, India.
Email: viceprincipal@klepharm.edu

Introduction

Psoriasis is a chronic inflammatory skin disease affecting more than 60 million people worldwide, including both adults and children [1]. Psoriasis significantly impacts a patient's physical, mental, and social health [2]. Topical medications are typically used to treat mild to moderate cutaneous psoriasis, although systemic therapy or phototherapy may be necessary for more severe cases. It has a substantial effect on one's bodily, social, or mental health, or it arises in specific regions, such as the face, genitalia, soles or palms [3]

Silver nanoparticles (AgNPs), together with polyphenols (flavonoids) exhibit promising anti-inflammatory effect. Polyphenol-coated silver nanoparticles exhibit strong anti-inflammatory action in the treatment of psoriasis by preventing the activation of nuclear factor-κB (NF-κB) in macrophages, which in turn inhibits the generation of pro-inflammatory cytokines [4]. AgNPs exhibit *in vivo* anti-inflammatory effects by suppressing NF-κB and pro-inflammatory mediators, enhancing anti-inflammatory molecules, selectively inhibiting cyclooxygenase (COX-2), and contributing to antioxidant activity [5].

The naturally occurring flavonoid kaempferol (KMP), 3,5,7-trihydroxy-2-(4-hydroxyphenyl)-4H-chromen-4-one), is found in various plant parts, such as seeds, leaves, fruits, flowers, and vegetables [6]. Tea, cabbage, beans, broccoli, tomatoes, grapes, strawberries, and medicinal plants like propolis contain KMP [7]. KMP was found to inhibit T-cell proliferation and attenuate mTOR signaling, suggesting its potential role as a novel mTOR inhibitor for the treatment of human psoriasis [8].

Quercetin (QRT), chemically known as 2-(3′,4′-dihydroxyphenyl)-3,5,7-trihydroxychromen-4-one, is a flavonol widely distributed in various fruits and vegetables. Several studies have demonstrated that QRT exhibits diverse biological activities, including immunomodulatory, antibacterial, antitumor, neuroprotective, antiallergic, antioxidant, and anti-inflammatory effects [9].

Liu et al. study reports that in the psoriatic skin lesion, kaempferol decreased CD3+ T cell infiltration and the gene expression of key pro-inflammatory cytokines, such as interleukin (IL)-6, IL-17A, and tumor necrosis factor (TNF)-α. Kaempferol reduced the proportion of IL-17A+CD4+ T cells in the lymph nodes and spleen of mice with psoriasis caused by IMQ. KMP inhibited T cell mTOR signaling and proliferation *in vitro* [8]. KMP nanoemulsion topical gel was prepared by Preeti et al., to improve the bioavailability of poorly water-soluble KMP to treat skin diseases [10]. Bhakti et al. study reveals nanoformulation bilosomal QRT gel exhibited better antipsoriatic activity compared to the conventional QRT gel [11]. Zhang et al. studied a liposome-in-gel system for topical QRT therapy, which shows good potential in psoriasis treatment [12].

Current first-line topical therapies for mild to moderate psoriasis include corticosteroids, vitamin D analogs and retinoids. However, corticosteroids cause skin atrophy and tachyphylaxis with prolonged use, vitamin D analogs and retinoids cause irritation [13,14]. Systemic therapies (methotrexate, biologicals) are reserved for severe cases due to cost and safety concerns [15,16]. These limitations underscore the need for an herbal, novel, safe, and effective topical alternative. Nanotechnology offers a promising approach to the bioavailability challenges of natural compounds through enhanced skin penetration via small particle size (<100 nm), protection from degradation, sustained drug release, and improved targeting to inflammatory sites [17]. Among metallic nanoparticles, silver nanoparticles (AgNPs) have gained attention due to their intrinsic anti-inflammatory and antimicrobial properties [18,19] .

Traditional chemical synthesis of AgNPs often involves toxic reducing agents (e.g., sodium borohydride) and capping agents (sodium citrate) that raise safety concerns for topical applications [20]. The use of plant- derived polyphenols like KMP enables nanoparticle formation through intrinsic reducing and capping properties, which may decrease toxicity and enhance biological compatibility

Despite the individual anti-psoriatic potential of KMP and QRT, studies investigating their combined co-delivery within nanoparticle-based topical gel systems remain limited. Despite having anti-inflammatory, antioxidant, and anticancer qualities, KMP has low bioavailability and poor water solubility, which frequently restricts its therapeutic efficacy [21]. To address these challenges, we developed a promising topical nano formulation of kaempferol-silver nanoparticle quercetin gel (KSNPs). There is currently no published data demonstrating the efficacy of KMP and QRT together in treating psoriasis infection and associated inflammation in an animal model that mimics psoriasis produced by imiquimod (IMQ). Therefore, we used an IMQ-induced animal model to demonstrate the efficacy of KSNPs-loaded QRT gel in this study. Also, the prepared formulation was evaluated for *in vitro* anti-psoriatic activity in the HaCaT human keratinocyte cell line, skin irritation, and *in vivo* anti-inflammatory and anti-psoriasis study.

Materials and Methods

Materials

Kaempferol (Purity 99.4%) was obtained from Chemical Book Inc. (China), while Quercetin (Purity 98 %), Carbopol 934, triethanolamine, and silver nitrate were purchased from SD Fine Chemicals (Gujarat, India). Sodium carbonate was procured from Merck (India). Imiquad 5% w/w imiquimod cream (Glenmark Pharmaceutical Ltd., India), Nobel Pain Relief Diclofenac gel (Lupin Ltd., India), topical clobetasol gel 0.05% w/w (Systopic Laboratories Pvt. Ltd., New Delhi), and Inmecine 1% w/w indomethacin gel (Sterkem Pharma Pvt. Ltd., India) were

obtained from a local pharmacy. The water used throughout the study was purified using a Millipore-Q purification system.

Ethical approval

The study was approved by the Institutional Animal Ethics Committee (IAEC), KLE College of Pharmacy, Belagavi (Ethical approval reference: 221/Po/Re/S/2000/CPCSEA Reg. No. 34). All animals were anesthetized using inhalational isoflurane to minimize pain and distress during experimental procedures, and humane euthanasia was performed under deep isoflurane anesthesia in accordance with CPCSEA guidelines for laboratory animal care and use.

Preparation of kaempferol-silver nanoparticle quercetin gel

One-pot synthesis of silver nanoparticles KSNPs

KMP 0.286 mg dissolved in 10 mL ethanol to form a homogenous solution with a concentration of 0.1 mmol/L. pH was adjusted to 8–9 with sodium carbonate. 10 ml KMP solution was added dropwise to an aqueous 100 ml $AgNO_3$ solution (1.2 mmol/L) with stirring at 50 °C. Incubate for 30 min. Formed nanoparticles were collected by centrifugation at 8000 rpm for 15 min, and the pellet was purified with double-distilled water. The washed pallet was kept in the oven at 34 °C to dry and stored in the refrigerator (2–8 °C) for further analysis. The reliability of this approach was confirmed after the experiment was replicated three times [22].

Characterization of silver nanoparticles

UV–Visible Spectroscopic Analysis

Synthesized KSNP were diluted with deionized water and scanned in a wavelength range of 200–800 nm using a UV-visible spectrophotometer (Shimadzu 1900, UV probe software) to confirm the formation of AgNPs and study surface plasmon resonance (SPR) effect.

Fourier-Transform Infrared Spectroscopy (FTIR)

FTIR analysis was performed to identify and study the chemical interactions between the excipients using a JASCO FTIR-4200 type A (Tokyo, Japan). IR-grade potassium bromide was mixed with 3 mg of each sample. Discs were created from compressed mixtures. The scanning was conducted in the 4000–400 cm^{-1} range. Study components such as KMP, silver nitrate and KSNP were used for the FTIR assessment.

XRD Analysis

Crystallinity of the prepared KSNPs with a resolution of 0.001 Å was measured using the X-ray diffractometer Bruker D2 Phaser, Germany. The device uses a copper anode to emit a monochromatic X-ray spectrum that passes through the sample vessel at 2θ between 3 and 160° while operating at 40kV and 30mÅ for 5 seconds.

Mean particle size, polydispersity index, and zeta potential measurement

The mean particle size, PDI, and zeta potential of KSNPs were measured using the dynamic light scattering mechanism of the Malvern ZS 90 Zetasizer device. At 25°C, the undiluted KSNP sample was placed in a glass cuvette and exposed to 90° of scattering light.

TEM analysis

Transmission Electron Microscopy (TEM) was used to illustrate the surface morphology and crystal geometry. A copper matrix covered in a carbon coating was gently treated with a drop of the KSNPs dispersion. After extracting the excess liquid using Whatman® filter paper, the sample was allowed to dry for 24 hours at room temperature (25°C). The material was analyzed using a JEOL JEM-F200 (Japan).

Formulation of KSNPs loaded QRT gel

The KSNP-loaded QRT gel was prepared using Carbopol 934 (1.5% w/w) as the gelling agent. To ensure proper polymer hydration, Carbopol was dispersed in Millipore-Q purified water and allowed to hydrate overnight. After preliminary optimization, QRT (25 mg) and KSNPs (0.175 mg) were incorporated into the gel base, and the final weight of the formulation was adjusted to 10 g. This corresponded to final concentrations of 0.25% w/w (2.5 mg/g) QRT and 0.00175% w/w (0.0175 mg/g) KSNPs. Methyl paraben (0.2% w/w) was used as a preservative, and the pH was adjusted to 7 using triethanolamine (0.02% w/w) under continuous stirring [23-25].

Characterization of Gel

FTIR of KSNP gel

FTIR analysis of gel was performed to identify and study the chemical interactions between the excipients using a JASCO FTIR-4200 type A (Tokyo, Japan). IR-grade potassium bromide was mixed with 3 mg of each sample. Discs were created from compressed mixtures. The scanning was conducted in the 4000–400 cm^{-1} range.

pH and Viscosity measurement

KSNP- QRT gel formulation was made, and its pH was measured using a pre-calibrated pH meter (Equiptronics EQ-610 pH meter, India). pH of the formulation was measured three times at 25±5°C. The viscosity of the prepared gel formulation was measured. The Brookfield viscometer's spindle number 64 (DVplus, Brookfield, AMETEK Inc., USA) was used to measure the viscosity of the created gel formulation. The spindle revolved at 50 rpm while a 100 g sample was removed for analysis. This was

carried out in triplicate at 25±5 °C.

Entrapment efficiency (EE)

The entrapment of KMP in KSNPs was assessed by calculating the % EE of produced KSNPs. The KSNPs sample was centrifuged for 30 minutes at 50 ˚C at 3000 rpm using a Remi India cooling centrifuge. KMP that was loaded by KSNPs settled at the bottom. At 413 nm, the unentrapped drug is still present in a supernatant that is decanted and measured using a spectrophotometer (Shimadzu UV 1800). The % EE was estimated using the following formula [26].

$$\%EE = \frac{Total\ Drug - Unentraped\ Drug}{Total\ Drug} \times 100$$

In vitro drug release study

Using the Franz diffusion cell, the selected KSNP release performance of the gel was examined over a period of 24 hours at various time intervals. Using a 10 mL Franz diffusion apparatus with an internal diameter of 10 mm, the receptor medium was phosphate buffer, pH 4.5, as a release medium. A previously soaked dialysis membrane in phosphate buffer 4.5 for 24 hours with a surface area of roughly 1.77 cm^2 was placed. The entire assembly was maintained at 37±2 °C over 300 rpm using a Remi 1 LMH Q-19 magnetic stirring device. The membrane was positioned between the donor and receptor compartments after a 1 g gel sample was placed on its surface. At predetermined intervals, 1 mL sample was removed from its receiving chamber and replaced with an equivalent volume of brand-new media. A UV spectrophotometer (Shimadzu UV 1800) was used to measure the amount of drug released [27].

In vitro anti-inflammatory activity

In vitro HRBC membrane stabilization study

Human red blood cells (HRBC) were used to measure the anti-inflammatory effectiveness of the formulation. Three healthy volunteers provided 2-3 ml of human blood. Alsever's solution (2% dextrose, 0.8% sodium citrate, 0.05% citric acid, and 0.42% sodium chloride in water) was combined with the blood in an equal volume. After centrifuging the mixture for 10 minutes at 3000 rpm, the supernatant was removed, and the packed cells were cleaned 3 times using an isosaline solution (0.9%, pH 7.2). 1 mL of phosphate buffer (pH 7.4), 2 mL of hyposaline solution (0.36%), and 0.5 mL of HRBC suspension (10% v/v) were combined with 1 mL of gel at different concentrations (125, 250, and 500 µg/mL) or reference medication diclofenac sodium (125, 250, and 500 µg/mL) to create the test combination. Phosphate buffer served as the blank, and distilled water was utilized as the control in a reaction mixture. After 30 minutes of incubation at 37 °C, the mixtures were centrifuged at 3000 rpm. Using spectrophotometry, the hemoglobin concentration of the supernatant solution was calculated at 560 nm[28] . The following formula was used to determine the HRBC membrane stabilization percentage:

$$Percentage\ of\ stabilization = \left(\frac{Absorbance\ of\ control - Absorbance\ of sample}{Absorbance\ of\ control}\right) \times 100$$

Inhibition of protein denaturation study

A mixture of 0.02 mL of the gel sample, 0.2 mL of 1% bovine albumin, and 4.78 mL of pH 6 PBS (phosphate buffer saline) was properly mixed. The mixture was then incubated for 15 minutes at 37 ˚C, heated in a water bath for 5 minutes at 70 °C, and cooled. Once the mixture cooled, its absorbance was measured using a UV spectrophotometer set to 660 nm. A solution of phosphate buffer is used as the control in this process [29]. The percentage of inhibition of the protein denaturation was calculated by using the following formula

$$Percentage\ of\ inhibition\ of\ denaturation = \frac{1 - Absorbance\ of\ sample}{Absorbance\ of\ control} \times 100$$

In vitro anti-psoriatic activity by Sulphorhodamine B (SRB) assay to study

The HaCaT human keratinocyte cell line was used to test for *in vitro* anti-psoriatic activity of KSNP-loaded QRT gel formulation. The cells were cultivated in Dulbecco's modified Eagle's medium after being seeded in a 96-well microtiter plate at a density of 1.0×10^5 cells/mL. Added 10% fetal bovine serum as a supplement. The supernatant was decanted, and the monolayer was washed once after 24 hours. The cells in microtitre plates were then exposed to 100 µL of the test material in different concentrations. The final concentration of DMSO in the culture medium was 0.2% after the test compounds were synthesized in dimethyl sulphoxide (DMSO). Three duplicate samples of each concentration were tested. DMSO was used as a control. Asiaticoside, a well-known triterpenoid saponin with documented anti-proliferative and anti-inflammatory effects on keratinocytes, was used as a positive control to benchmark the anti-psoriatic activity of the KSNP-quercetin gel formulation[30]. After that, the plates were incubated for 3 days at 37 °C in an environment with 5% CO_2. Sulphorhodamine B (SRB) assay was used to measure anti-proliferative activity. Following an hour of incubation at 4 °C, cells were fixed by adding 25 µL of ice-cold 50% trichloroacetic acid on top of the growing media. The plates were then rinsed to get rid of any remaining media, medication, and serum. Each well was filled with 50 µL of SRB stain (0.4%) in 1% acetic acid. The cells were then allowed to contact with the stain for 30 minutes. They were then rinsed four times with 1% acetic acid until only the dye that was stuck to the cells remained. To solubilize the dye, 100 µL of 10 mM Tris was added to each well of the dried plates. The plates

were then gently shaken for five minutes, and a microplate reader was used to measure absorbance at 550 nm [30,31].

Skin irritation study

The Draize skin irritancy detection test was used to assess the irritancy potential of the prepared KSNPs-loaded QRT gel. The study included male Wistar rats (weighing between 150 and 200g). The test sample of KSNP-loaded QRT gel was applied uniformly to a 1 cm × 1 cm area to the left ear of the animal; while the right ear served as an untreated control. The animals were checked for signs of erythema or edema 24 hours, 48 hours, 72 hours, and on the 7th day following administration, and scored using the Draize method [32,33].

In vivo anti-inflammatory activity

The *in vivo* anti-inflammatory activities of the prepared KSNP-loaded QRT gel were investigated using a carrageenan-induced paw edema model in Wistar rats. 0.1 mL of 1% w/v carrageenan was subcutaneously injected into the sub-plantar tissues of each rat's left hind paw to cause paw edema. Three groups of 6 Wistar rats (weighing 150–200 g each) were randomly selected. Carrageenan 1%, 0.1 mL were given subcutaneously to Group I, the diseased control; Group II received standard treatment, which is a commercialized formulation of 1% w/w Indomethacin gel; and Group III received carrageenan and KSNP-loaded QRT gel, applied topically. The paw thickness was measured using a plethysmometer before the carrageenan infusion as well as after 60, 120, 180, and 240 minutes [34,35] The % inhibition of edema was estimated using the formula.

$$\% \text{ Inhibition} = \frac{To - Tt}{To} \times 100$$

where, Tt is the thickness of the paw of rats receiving formulations to be tested at the corresponding time, and To is the paw thickness of rats of the control group at the same time.

IMQ-induced psoriasis-like animal model

Male Wistar rats weighing 150–200 g were used as experimental animal model to evaluate the anti-psoriatic efficacy of KSNP-loaded QRT gel. Animals were randomly allocated into four groups (n = 6 per group). The animals were provided with standard laboratory feed and had constant access to water. Psoriasis-like skin inflammation was induced by the topical application of 125 mg of commercially available 5% imiquimod (IMQ) cream (Imiquad®, Glenmark Pharmaceuticals Ltd., India) once daily for six consecutive days on a defined 1 cm² area on the dorsal surface of the left ear of Wistar rats. Following disease induction, IMQ application was discontinued, and animals received topical treatment once daily for a total duration of 14 days. Group I served as the normal control, group II as the disease control (IMQ only), group III received IMQ followed by 1% clobetasone treatment, and group IV received IMQ followed by KSNP-loaded quercetin gel treatment. The KSNP-loaded QRT gel was applied topically once daily (five applications per week) for two weeks at a dose of 2 mg/cm², corresponding to approximately 5 µg of quercetin and 0.035 µg of KSNPs per treated area. The formulation was applied uniformly using a sterile spatula to ensure consistent coverage [32].

Scoring the severity of psoriatic skin inflammation

The severity of psoriatic skin inflammation was evaluated using the Psoriatic Area and Severity Index (PASI) guidelines. Psoriasis scoring tables were employed to assign individual scores for erythema, scaling, and thickness, with values ranging from 0 (none), 1 (slight), 2 (moderate), 3 (marked), to 4 (very marked). Ear thickness was measured using digital calipers, where an increase was considered indicative of both epidermal hyperproliferation and inflammatory response. At the end of the experimental period, rats were sacrificed, and ear skin samples were collected for further analysis [36].

Histopathological study

The histopathology of the ear pinna of Wistar rats was examined. Once the specified 14-day treatment period was completed, the proper set of animals were sacrificed. The ears were cut into thin, vertical slices after being fixed in a 10% v/v formalin solution. Sections were then stained with eosin and hematoxylin dye. An optical microscope was used to examine the dyed ear segments on the glass slides.

Stability study

The formulated KSNP-loaded QRT gel was maintained at room temperature (25±2°C, 60±5% RH) and at accelerated temperature conditions (40±2°C, 75±5% RH) for three months. Triplicate measurements of pH, viscosity, spreadability, and encapsulation efficiency were made at predetermined intervals.

Cytotoxicity and cell viability study

The cells were seeded in a 96-well flat-bottom microplate with 5% CO_2 and 95% humidity at 37 ºC for the entire night. The concentrations of the samples used for the treatment were 100, 50, 25, 12.5, 6.25, and 3.125 µg/mL. Cells were incubated for forty-eight hours. Twenty microliters of the MTT staining solution were applied to each well after the wells had been cleaned twice with PBS, and the plate was then incubated at 37 °C. Each well received 100 µL of DMSO after 4 hours to dissolve the formazan crystals, and a microplate reader was used to measure absorbance at 570 nm.

$$\text{Surviving cells (\%)} = \frac{\text{Mean OD of test compound}}{\text{Mean OD of Negative control}} \times 100$$

Result and Discussion

Preparation of Kaempferol-Silver Nanoparticle Quercetin Gel

Preparation of KMP-Silver Nanoparticle

KMP, a flavonoid produced from plants, was effectively used to formulate KSNPs. The development of KSNPs is indicated by the color of the solution changing from colorless or light yellow to reddish brown. There are several steps involved in the development of nanoparticles, including the reduction of silver ions, the nucleation process, and finally the synthesis of nanoparticles. KMP-silver nanoparticle was prepared successfully as per the procedure mentioned in the methods section.

Characterization of KSNP

UV Visible spectroscopic analysis

UV–Visible spectra were recorded using a UV–Visible spectrophotometer over the wavelength range of 200–800 nm. The KSNP spectrum was recorded after completion of nanoparticle synthesis.

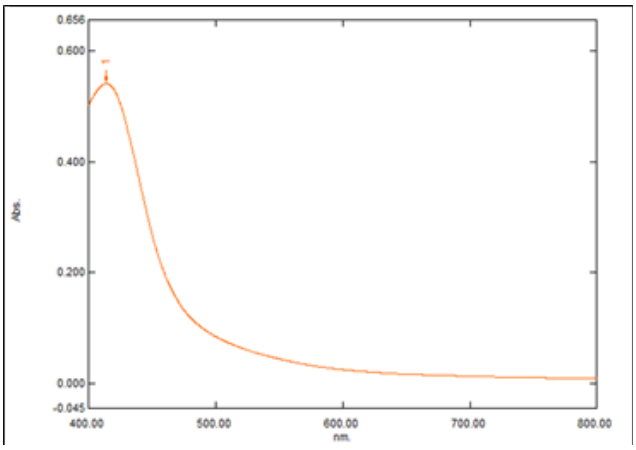

Figure 1. UV-visible spectra of silver nanoparticles (KSNP)

The UV–Visible spectrum of KSNPs exhibited a characteristic absorption peak at 414.20nm (Figure 1), which corresponds to the SPR band of silver nanoparticles. The presence of this SPR peak confirms the successful formation of silver nanoparticles. The broad nature of the absorption band suggests nanoscale particle formation with possible size distribution and surface interaction with kaempferol acting as a stabilizing agent.

FTIR Study

The FT-IR spectrum of the KMP-mediated silver nanoparticles (Figure 2) exhibited characteristic absorption bands indicating the involvement of KMP functional groups in the reduction and stabilization of the nanoparticles. A broad absorption band observed in the region around 3400–3300 cm^{-1} corresponds to the stretching vibrations of phenolic O–H groups. Compared with the pure KMP spectrum, this band appears slightly broadened and shifted, suggesting the participation of hydroxyl groups in the reduction of Ag^{+} ions and their subsequent interaction with the nanoparticle surface through hydrogen bonding or coordination. Weak bands observed in the region of 2900–2700 cm^{-1} may be attributed to overtone or combination bands, as well as minor environmental contributions. The characteristic carbonyl stretching vibration of the flavanol structure appears around 1650–1600 cm^{-1}; however, in the nanoparticle spectrum, this band shows a slight shift and change in intensity, indicating the involvement of the conjugated C=O group in coordination with silver ions. The peaks in the region of 1600–1400 cm^{-1} correspond to aromatic C=C stretching vibrations, which are retained but show minor shifts, suggesting interaction between the aromatic system and the nanoparticle surface. In the fingerprint region, prominent bands between 1300 and 1000 cm^{-1} are attributed to C–O stretching vibrations of phenolic and ether groups. Slight shifts and intensity variations in these bands compared with pure KMP indicate the binding of these oxygen-containing functional groups to the silver nanoparticle surface, acting as capping and stabilizing agents. Additional peaks observed around 850–800 cm^{-1} correspond to out-of-plane bending vibrations of aromatic C–H bonds.

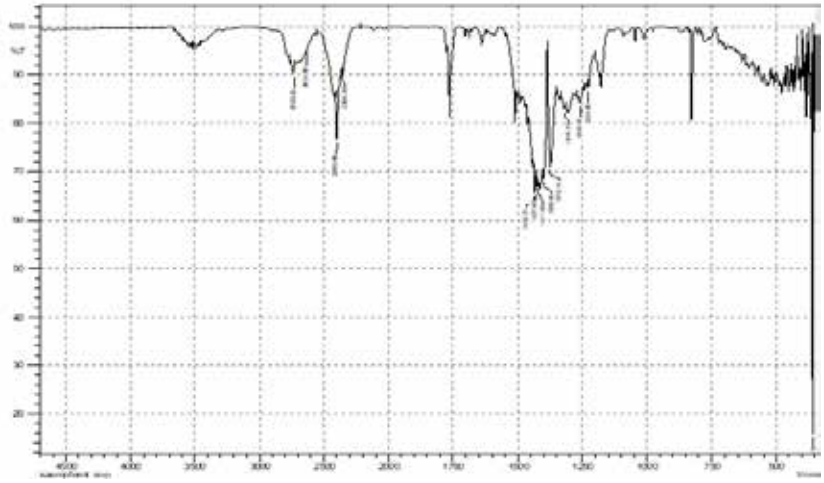

Figure 2. FTIR spectra of Kaempferol Silver nanoparticle

XRD Analysis

The crystalline shape of KSNPs was verified by an XRD analysis, as per Yue Tian et. al.'s studies [37] The X-ray diffraction pattern of KSNPs is shown in Figure 6 S. KMP and Silver both showed their characteristic strong peaks in the XRD pattern of the KSNP, indicating the crystalline nature of KSNPs. In addition to the typical Bragg's peak at 34 and 45 in this instance, additional spikes were seen, indicating that the KMP aggregation formed on the outermost layer of the SNPs.

Particle size and zeta potential

The particle size and zeta potential of KSNPs are shown in Figure 7 S and Figure 8 S, respectively. While electrostatic repulsion aids in stabilizing KSNPs, which is investigated by measuring the zeta potential, and was shown to be -39.2 mV. Bio-reduction of silver nitrate using sodium carbonate helps to regulate the particle size to 113.2 nm. The coating of the phytochemicals in KMP that contain hydroxyl groups and are employed to reduce and stabilize KSNPs may be the cause of the negative zeta potential of KSNPs. It is the responsibility of these phytoconstituents to give SNPs a strong covering, which prevents aggregation. With a PDI of 0.241, the KSNPs particle size was found to be 113.2 nm.

Zeta potential is an important parameter that describes the stability of colloidal dispersion. Its magnitude can be used to estimate this stability. The symmetry of the attractive and repulsive interactions between SNPs is indicated by this scale. The number of repulsive forces between SNPs and the number of attractive forces between them are closely correlated with stability. The current study determined that the zeta potential of the KSNP was found to be -39.2 mV. It helped lower and stabilize the SNPs, and the coating of the hydroxyl group found in the KMP molecular structure may be the cause of the negative zeta potential of SNPs. In an alkaline environment, the KMP molecule becomes a stronger reducing mediator to convert Ag^{+} to Ag^{0} and ultimately nano-Ag by losing a hydrogen atom in its hydroxyl functional group. However, it also becomes a stronger complexing mediator for Ag^{+} ions [38]. Consequently, in accordance with current studies in this area, the KMP molecule may both create SNPs and stick to their surface to provide them stability.

TEM analysis

The graphics produced by analyzing the aqueous dispersion of KSNPs are shown in Figure 9 S. The KSNPs are found in clusters with high frequency and polydispersity. Small-diameter particles were the most common. The KMP molecules adsorbed on the Ag surface are displayed in Figure 9 S. In an alkaline environment, the KMP molecule becomes a more powerful reducing mediator by losing a hydrogen atom in the hydroxyl functional group, which transforms Ag^{+} into Ag^{0} and eventually nano Ag. It also becomes a stronger complexing mediator for Ag^{+} ions, on the other hand. The KMP molecule may adhere to its surface, stabilize it, and produce SNP all at once. These findings align with those published by Khalil et al. [39].

Characterization of Gel

FTIR Study of Gel

The IR spectrum of the kaempferol–silver nanoparticles incorporated with quercetin gel (Figure 1 S) exhibits distinct absorption bands corresponding to hydroxyl, aromatic, and metal–ligand functional groups, confirming successful interaction of the phytochemicals with silver nanoparticles and the gel matrix. A broad and intense absorption band observed around 3317 cm^{-1} is attributed to the stretching vibration of hydroxyl (–OH) groups from kaempferol, quercetin, and the gel base (Carbopol 934), indicating strong intermolecular hydrogen bonding and possible involvement of phenolic –OH groups in the reduction and stabilization (capping) of silver nanoparticles. The absence or weakening of free –OH sharp peaks compared to pure compounds suggests coordination of these groups with the SNPs surface. Bands appearing in the region 1658–1629 cm^{-1} correspond to C=O stretching and aromatic C=C stretching vibrations of the flavonoid structure, confirming the presence of conjugated carbonyl and benzene ring systems. The peaks at approximately 1547 cm^{-1} and 1491 cm^{-1} are assigned to aromatic C=C stretching vibrations, further supporting the retention of the flavonoid framework after nanoparticle formation and gel incorporation. Additional bands between 1390 and 1030 cm^{-1} correspond to C–O stretching vibrations of phenolic and carboxylic groups as well as polymer backbone vibrations, suggesting physical interactions and stabilization within the gel matrix. Overall, the spectral profile suggests successful incorporation of kaempferol-mediated silver nanoparticles and quercetin into the Carbopol gel without significant chemical incompatibility. Supporting data of FTIR of QRT (Figure 2S), KMP (Figure 3S), silver nitrate (Figure 4S), and Carbopol 934 (Figure 5S) is given in the supplementary.

pH and Viscosity measurement

The formulated gel has a pH of 6.50 ± 0.01, which is within the natural skin pH range, indicating good skin compatibility and a lower risk of irritation when applied topically. Its viscosity, measured at 1165± 2.00 cP, reflects suitable rheological properties that ensure the gel remains at the application site while allowing for easy and controlled spreading. These characteristics confirm the formulation's appropriateness for topical use, offering desirable stability and user acceptability.

Entrapment efficiency

The study found that as the polymer concentration increased, the entrapment efficiency of KSNPs increased

from 85.76 ± 3.63 to 89.54 ± 1.27. The greatest entrapment efficiency was demonstrated by the formulation. During the synthesis and stability of the polymer, nanoparticles have a propensity to conjugate with its functional units. Additionally, this contributes to the stability of the matrix. The % EE characteristics drop as a result of the drug's potential to slip out of its conjugation with silver molecules during gel formation. The stable silver-KMP complex is the cause of the increase in the % EE.

Drug release study

This study was performed with the primary goals of examining the drug release behavior of KSNP – quercetin gel and free KMP solution, and comparing the drug release kinetics with the clobetasone gel, which was chosen as a commercial formulation. Within five hours, the free KMP solution showed more than 87% drug release, whereas the produced KSNP gel showed 85.15%, and the commercial formulation showed 62.69% cumulative drug release over 24 hours. Figure 10 S shows the results of the drug release study. Formulated gel showed a slower, controlled release with a gradual increase over ~24 hours, reaching 85.15%. Free KMP showed a rapid release reaching nearly 100% within a few hours. This is characteristic of immediate release, typical of a first-order or burst release for a freely soluble drug; while clobetasol gel showed a slower, sustained release, plateauing around 60% after ~24 hours. The drug release kinetics of KMP SNP Gel were evaluated using Zero-order, First-order, Higuchi, and Korsmeyer–Peppas models. The Higuchi model showed the best correlation (R^2=0.982), confirming that drug release was primarily diffusion-controlled. Overall, the release profile demonstrated a controlled and sustained mechanism suitable for topical application.

In vitro anti-inflammatory activity

Reactive oxygen species and cytokines work together to trigger an inflammatory response that may prevent healing and complicate psoriasis treatment. The results of an anti-inflammatory investigation using the bovine serum protein denaturation method are shown in Figure 11 S. The KSNP-loaded QRT Gel at concentrations of 100, 200, 300, 400, and 500 µg/ml demonstrated 41.59%, 61.70%, 63.26%, 68.66%, and 77.55 % inhibition of denaturation of bovine serum, respectively. Standard therapy of DS confirmed 41.27%, 54.97%, 62.62%, 66.10%, and 73.43 % prevention of denaturation of bovine serum. The human red blood cell membrane stabilization method was also performed to evaluate the anti-inflammatory potential of the prepared formulation, and the results are shown in Figure 12 S. and DS displayed a dose-dependent reaction. It has been noted that increasing the dose improves membrane stability. RBC hemolysis was inhibited by 500µg/ml KSNP-loaded QRT gel at 57.27 ± 3.54 and 500µg/ml DS at 21.05 ± 4.36 percent. We can infer from the above-mentioned results that the KSNP-loaded QRT gel exhibits greater anti-inflammatory activity than the conventional DS therapy.

In vitro Anti-psoriasis activity

The HaCaT Cell line study was carried out effectively for the percentage cell viability at different concentrations between 6.25 µg/mL and 100 µg/mL. The conventional medication Asiaticoside and the untreated HaCaT cell line were used to compare the study. According to the study's findings, the percentage of HaCaT cells that survive drops as the test formulation's concentration rises. The lowest cell viability in the MTT experiment was observed at 100 µg/ml, which showed 30.77%. This was followed by 50 µg/mL, which showed 64.28%, and similarly, 25 µg/mL, 12.5µg/mL, and 6.25 µg/mL, which showed 80.88%, 87.26%, and 93.41%. 30.77% cell viability is shown in the experimental gel as depicted in Figure 13 S. With a cell viability percentage of 30.77%, this study demonstrates the superiority of the formulation. According to the study's findings, prepared gel is more efficient, and KMP possesses the ability to trigger stress proteins and oxidative stress-mediated cell death.

Skin irritation study

The erythemal ratings that were observed were used to assess the likelihood of skin irritation. According to the findings, there was no erhythmal evidence on the skin following a 24-hour topical application of the KSNP-loaded QRT formulation. The developed formulation is safe to use and may not cause any kind of hypersensitive reaction when applied, with respect to the study.

In vivo Anti-inflammatory activity

The carrageenan-induced paw edema model is a classical method to evaluate acute inflammation. The results of this study, in Figure 3, show how the paw volume increased over time after the carrageenan injection. The greatest amount of paw edema (0.95 mL formulation) was noted 2 hours following delivery. But as Figure 4 illustrates, carrageenan-induced paw edema was much lessened by treatment with the designed formulation and commercially available indomethacin gel in a dose-dependent manner. By 62.03% during the 12th hour, formulation dramatically decreased paw edema. Also, standard indomethacin gel significantly reduced paw edema by 49.07%. Disease control group I showed a progressive increase in paw volume, confirming successful induction of inflammation. Standard treatment group II reduced inflammation through COX inhibition, consistent with its known mechanism of action. KSNP-loaded QRT Gel Group III showed that the superior anti-inflammatory activity of the KSNP-QRT gel can be attributed to KSNP' ability to enhance the skin penetration and bioavailability of QRT. The pharmacological action of QRT includes the inhibition of inflammatory mediators and free radical scavenging [40,41]. The same outcomes may be seen in

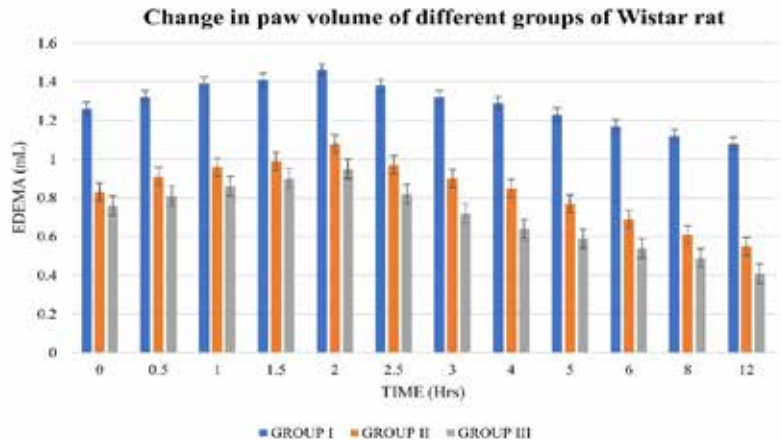

Figure 3. Graph showing the change in paw volume in different groups of Wistar rats

the photos (Fig.4). It is evident that the experimental formulation exhibited superior activity in comparison to the conventional indomethacin gel.

IMQ induces psoriasis model & In vivo Anti-psoriatic activity

To investigate the efficacy of manufactured KSNPs-loaded QRT gel against psoriasis and associated inflammation throughout the period of seven days to fourteen days, the IMQ-induced psoriasis model was studied as per the study protocol stated by Mestry et al. in their research investigation, taking into account psoriasis area, PASI score, and related histology. According to the results of the H&E analysis, Wistar rats' ear tissues exhibit markedly higher levels of acanthosis, hyperkeratosis, and inflammatory reactions when they have psoriasis brought on by IMQ [42]. In order to score psoriasis, factors like erythema, scaling, and thickness were taken into account. When compared to the control group (group I), the positive control (group II) animals displayed the highest rating, indicating an inflammatory response. When compared to the third animal group that got a commercially available version of clobetasone 1% cream, the Group IV animals who received the KSNPs-loaded QRT gel formulation demonstrated a comparatively significant decrease in inflammation. When compared to group III animals treated with the marketed product, animals treated with KSNPs-loaded QRT gel demonstrated recovery from the 9th to the 14th day. Histopathological analysis was carried out on the 7th and 14th days of normal, positive control, animals treated with commercial preparation, and the group of animals treated with KSNPs, as depicted in Figure 5. Normal skin showed normal dermal, epidermal, and hair follicle anatomy. Animals with psoriasis have erythematous skin with inflammation-related symptoms. Skin thickening occurs together with keratinocyte hyperpigmentation and keratin accumulation. While the animals in the KSNPs-treated group recovered quickly from the 9th day of treatment and their normal skin structure was restored by 14th day of treatment, the animals in the clobetasone-treated group

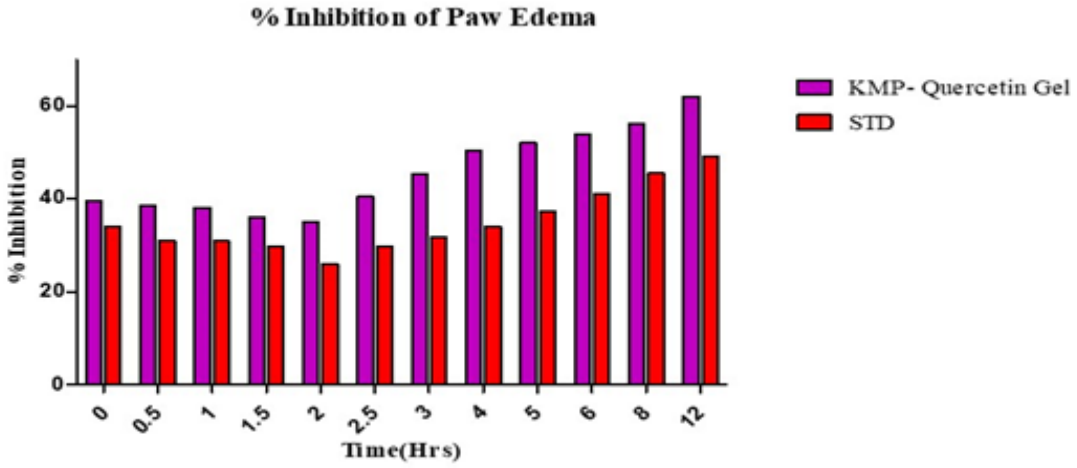

Figure 4. Graph showing the comparative % inhibition of paw oedema of optimized KSNP-loaded KMP gel and Indomethacin gel as a standard

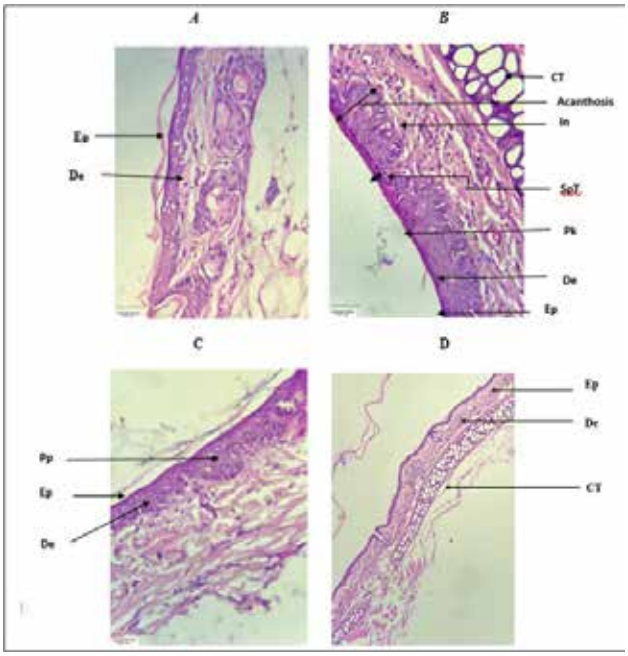

Figure 5. Longitudinal histological sections of the ear of a Wistar rat treated topically, hematoxylin and eosin staining. A: Normal control; B:Positive control; C:Treated ear ; D:Experimental gel treated ear (A) Normal control: represents normal epidermis (Ep) and dermis (De); (B) Positive control (IMQ) treated ear: represents Suprapapillary thinning (SpT), Acanthosis, parakeratosis (Pk)and presence of inflammatory cells (In) in the dermis region, represents normal epidermis (Ep), dermis (De), and cartilage (CT); (C)treated ear: reduced hyperplastic epidermis (Ep), the reduced presence of inflammatory cells (In) in the dermis region

still displayed significant psoriasis symptoms. Stress protein synthesis, microtubule and mitochondrial disintegration, cytochrome c release, and caspase activation can all lead to KMP-mediated cell arrest and its nanoscale size, which may be the cause of the return of normal skin structure and decrease in inflammation [42,43]

Scoring the severity of psoriatic skin inflammation

The severity of psoriasis-like lesions was evaluated using a modified PASI scoring system based on erythema, scaling, and skin thickness. The disease control group (IMQ) exhibited a significantly elevated PASI score (10.83 ± 0.75), confirming successful induction of psoriasis-like inflammation compared to the normal control group (0.00 ± 0.00). Treatment with 1% clobetasone (standard group) resulted in a significant reduction in PASI score (5.16 ± 0.75) compared to the disease control group (p<0.001), indicating therapeutic improvement. Notably, animals treated with the KSNP-QRT gel (experimental group) showed a further decrease in PASI score (2.66 ± 0.81), demonstrating enhanced anti-psoriatic efficacy.

Statistical analysis using one-way ANOVA followed by Tukey's multiple comparison test revealed significant differences among all groups (p<0.001). The experimental treatment group exhibited significantly lower PASI scores compared to both the disease control and standard treatment groups, suggesting superior therapeutic effectiveness of the KSNP-QRT gel in reducing psoriasis severity.

Histology study

Histological analysis of longitudinal ear sections from Wistar rats stained with haematoxylin and eosin revealed distinct morphological changes across experimental groups. Group A (normal control) showed distinct epidermis (Ep) and dermis (De) that appeared intact and well-organized, with no signs of hyperplasia, inflammation, or structural abnormalities. In group B (positive control – IMQ-treated), marked pathological alterations were observed, including Suprapapillary thinning (SpT), acanthosis (epidermal hyperplasia), parakeratosis (Pk), indicating abnormal keratinization, dense infiltration of inflammatory cells (In) within the dermis, presence of cartilage (CT) beneath the dermal layer. These features are consistent with psoriasis induced by IMQ. Group C (treated ear), compared to the positive control, this group showed: Reduced epidermal hyperplasia and decreased inflammatory cell infiltration in the dermis. The tissue showed partial restoration of normal architecture, suggesting therapeutic efficacy of the treatment. Histological section of group D (experimental gel treated ear) revealed further reduction in epidermal hyperplasia compared to group C, and minimal inflammatory cell presence in the dermis. These findings indicate enhanced anti-inflammatory and anti-proliferative effects of the experimental gel formulation. The study demonstrates that topical application of the experimental gel significantly ameliorates IMQ-induced psoriasis in Wistar rats. Histopathological analysis revealed marked reductions in epidermal hyperplasia and dermal inflammatory infiltration, indicating both anti-proliferative and anti-inflammatory effects. Compared to the untreated and 1% clobetasone gel-treated groups, the experimental gel achieved superior restoration of normal skin architecture. These findings suggest promising therapeutic potential for the gel formulation in managing psoriasis-like skin conditions and warrant further investigation through clinical and mechanistic studies.

Cytotoxicity and cell viability study

In order to calculate the IC_{50} value, MCF-7 and L929 cell lines were chosen. Various concentrations of prepared gel formulations, such as 3.125, 6.25, 12.5, 25, 50, and 100 µg/ml, were used to measure cell viability. The comparative IC_{50} analysis confirmed distinct cytotoxic profiles of QRT, KMP, KSNP, KSNP-QRT gel, and doxorubicin (Dox) against MCF-7 cells and L929 cells. Among all tested formulations, the KSNP-QRT gel displayed the lowest IC_{50} value against MCF-7 cells (13.65

µg/mL), indicating the strongest antiproliferative activity, followed by Dox (24.82 µg/mL), KSNP (35.76 µg/mL), KMP (63.00 µg/mL), and QRT (66.87 µg/mL) On the other hand, KSNP- QRT gel presented the highest IC_{50} in L929 cells (99.96 µg/mL), indicating improved safety compared with QRT, KMP, KSNP and Dox.

The results shown in Figure 6 depict that the formulation has IC_{50} value was lower than QRT, KMP, KSNP's with respect to MCF cell lines.

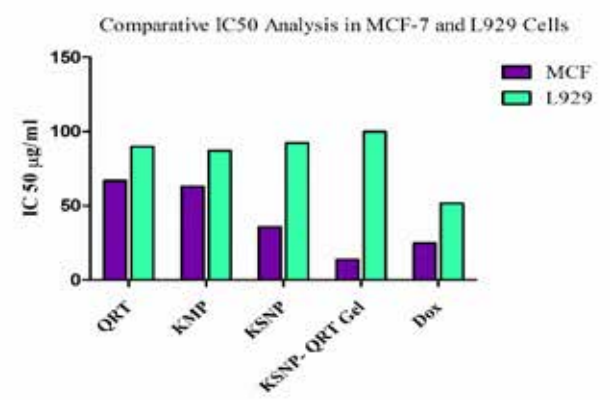

Figure 6. Experimental gel treated ear: reduced as compared to group C hyperplastic epidermis (Ep) and reduced presence of inflammatory cells, D. Cytotoxic activity of QRT, KMP, KSNP, KSNP + QRT gel and Doxorubicin on MCF and L929 Cell line

Stability study

The stability study of the optimized formulation is displayed in Table 1. The percent EE changed from an initial 89.54 ± 1.27% to 89.70 ± 0.08% at room temperature (25±2°C, 60±5% RH) after 90 days, and from 89.04 ± 0.09% to 89.78 ± 0.12% at accelerated temperature (40±2°C, 75±5% RH) after 90 days. This ensures factual accuracy and reproducibility of the stability assessment. The prepared SNPs with high surface charge caused repulsive interactions between them, preventing them from aggregating. As expected, the modified formulation's pH, viscosity, spreadability, and %EE changed marginally but not much after three months of sample retention. Larger particles settled in the newly created formulation, causing a discernible drop in spreadability and a subsequent increase in viscosity. It was discovered that KMP ejection had decreased. This characteristic resulted from an uneven crystal structure that provided an additional surface for trapping of the KMP in KSNPs.

Strengths and Limitations

The main benefits of utilizing herbal gels for psoriasis over synthetic drugs include less side effects, a more holistic approach to treatment, and more patient compliance. This study successfully developed and evaluated a novel KSNP-QRT gel for psoriasis management. The key findings demonstrate successful synthesis of stable KSNPs with high entrapment efficiency (89.54%), sustained drug release profile (85.15% over 24 hours), significant *in vitro* anti-inflammatory activity, minimal skin irritation, and marked reduction in psoriasis severity in the IMQ-induced rat model as evidenced by decreased PASI scores and histopathological improvements.

A limitation of the present study is the absence of a vehicle gel–treated control group in the IMQ-induced psoriasis model. Although carbopol-based gels are generally regarded as inert carriers with no inherent anti-psoriatic or anti-inflammatory activity, inclusion of a vehicle control would have allowed more precise attribution of therapeutic effects exclusively to the active nano formulation. Nevertheless, the significantly greater improvement observed with the KSNP-QRT gel compared to both the disease control and the standard clobetasone-treated group strongly suggests that the therapeutic efficacy arises from the action of KMP, QRT, and SNPs. Future studies will incorporate a vehicle control to further validate these findings.

Although the KSNP-QRT gel demonstrated superior therapeutic efficacy in both *in vitro* and *in vivo* models, the present study did not include single-agent KMP-only or QRT-only gel treatment groups in the IMQ-induced psoriasis model. Therefore, while the observed effects are consistent with the complementary pharmacological actions of KMP and QRT reported in the literature, definitive conclusions regarding pharmacological synergy

Table 1. Stability study of KSNPs loaded QRT gel

Parameters	Initial	Room temperature 25 ^{O}C ±2 ^{O}C/RH 60±5%			Accelerated temperature 40^{O}C ±2^{O}C/RH 75±5%			
Day		30th	60th	90th	Initial	30th	60th	90th
pH	6.50 ± 0.01	6.52± 0.01	6.51± 0.01	6.58± 0.01	6.51± 0.01	6.55± 0.01	6.54± 0.01	6.51± 0.01
Viscosity (cp)	1165± 2.00	1162± 2.00	1171± 3.00	1062± 4.00	1167± 3.00	1162± 3.00	1168± 3.00	1163± 2.00
Spreadability (g.cm/s)	6.23± 0.02	6.19± 0.01	6.26± 0.02	6.24± 0.02	6.12± 0.02	6.17± 0.02	6.09± 0.02	6.03± 0.02
% EE	89.54± 1.27	88.55± 0.10	89.13± 0.04	89.70± 0.08	89.04± 0.09	89.26± 0.19	88.34± 0.23	89.78± 0.12

cannot be drawn from the current data. Future studies incorporating individual component controls and combination index analyses will be required to quantitatively establish synergistic interactions.

Conclusion

Our goal was to prepare a rationally better nanomedicine to treat psoriasis. SNPs were created in the current investigation utilizing the quick one-pot synthesis approach using KMP. The formation of KSNPs was evidenced by the reduction of silver nitrate due to the inherent reduction capacity of the flavonoids. The synthesis of KSNPs in aqueous solutions is confirmed by the UV-VIS spectra. Zeta potential was measured to determine the stability of the synthesized silver nanoparticles, and a negative zeta potential of -39.2 mV indicates the formation of stable nanoparticles. The synthesized KSNPs showed a small particle size of 113.2nm with a 0.241 polydispersity index, which enhances drug permeation across the biological membrane. TEM investigation revealed a spherical shape with consistently rough surfaces and a high percentage of EE (89.54±1.27). The successful loading of KMP into KSNPs was confirmed by FTIR analysis, which revealed different changes, shifting, and the appearance or disappearance of distinctive peaks; XRD analysis, which revealed particular changes between crystalline and amorphous form; and KSNPs loaded QRT gel, which demonstrated early stabilization of the skin's epithelium layer in diseased animals in comparison to the group of animals treated with clobetasone. According to storage stability research, KSNPs-QRT gel does not significantly change its colloidal properties over 90 days of storage at ambient temperature or in a refrigerator. This study provides a theoretical basis for expanding the treatment combination of KMP and QRT in dermatological drug delivery systems and for developing novel psoriasis treatment approaches, thereby offering a promising prospect for improved therapeutic outcomes.

The study successfully formulated a stable KSNP-loaded quercetin gel. This gel exhibited superior anti-inflammatory and anti-psoriatic activity in both *in vitro* and *in vivo* models compared to conventional therapies. By enhancing skin penetration, improving quercetin bioavailability, and maintaining formulation stability, it provides a strong theoretical foundation for innovative psoriasis treatment strategies and highlights its potential for further clinical evaluation.

Conflict of Interests

None.

Acknowledgements

None.

Supplementary

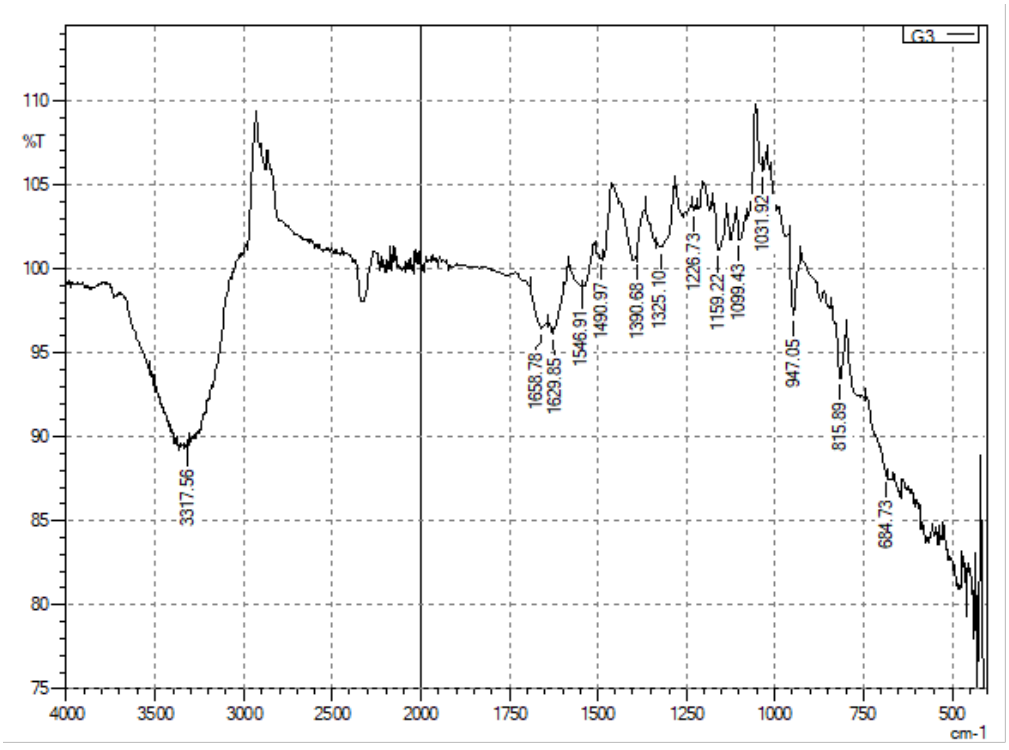

Figure 1 S. FTIR spectra of KSNP-QRT Gel formulation

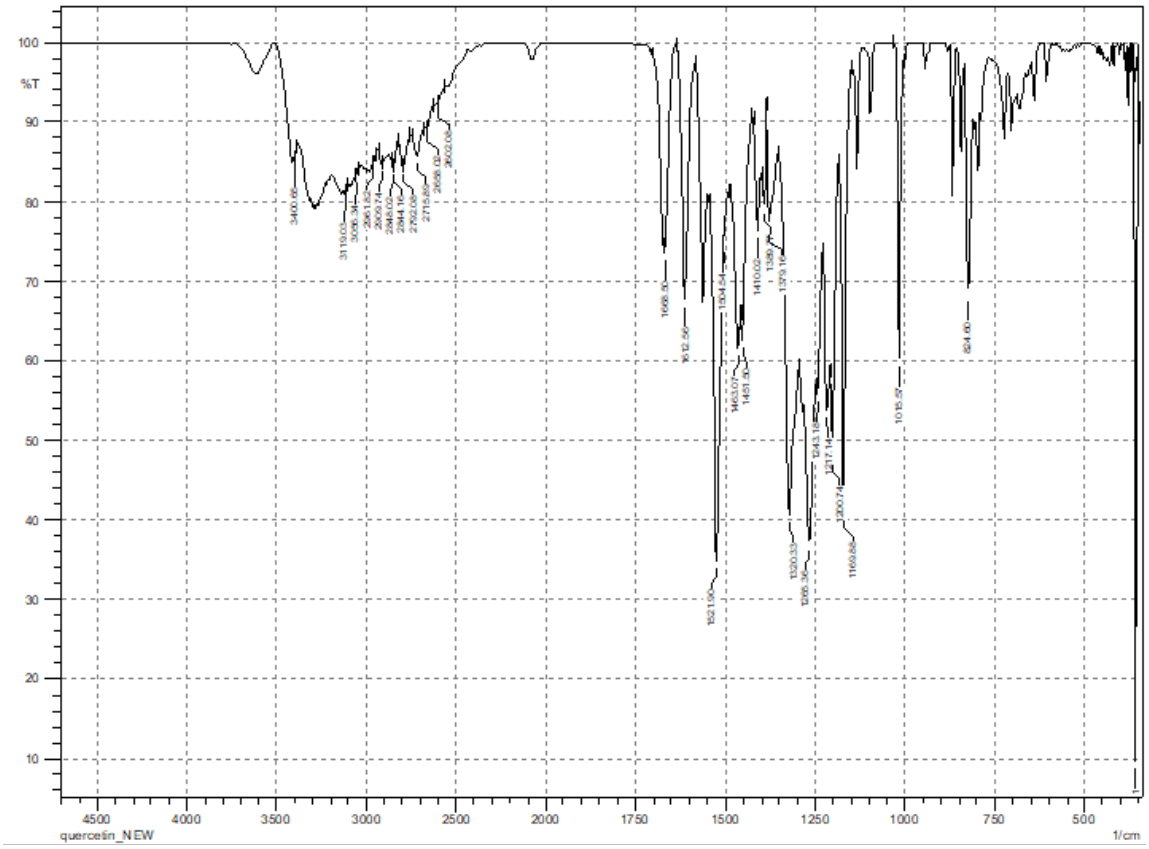

Figure 2 S. FTIR spectra of

The infrared (IR) spectrum of quercetin shows characteristic absorption bands that confirm the presence of multiple hydroxyl groups, aromatic rings, and a conjugated carbonyl system typical of flavonoids. A broad and intense absorption band observed in the region of approximately 3400–3200 cm^{-1} corresponds to the stretching vibrations of phenolic O–H groups, indicating extensive hydrogen bonding among the hydroxyl functionalities. Weak to moderate bands appearing around 3050–3000 cm^{-1} are assigned to aromatic C–H stretching vibrations, while bands in the region of 2920–2850 cm^{-1} may be attributed to minor aliphatic C–H stretching. A strong and sharp absorption near 1660–1650 cm^{-1} is characteristic of the conjugated carbonyl (C=O) stretching vibration of the flavone structure, confirming the presence of the ketone group at position C4. The prominent bands in the region 1600–1500 cm^{-1} arise from aromatic C=C stretching vibrations of the benzene rings, reflecting the polyphenolic aromatic framework of quercetin. Additional bands around 1450–1400 cm^{-1} are associated with C–H bending and phenolic O–H in-plane bending vibrations. The intense absorptions observed between 1300 and 1000 cm^{-1} correspond to C–O stretching vibrations of phenolic and alcoholic groups as well as C–O–C stretching within the heterocyclic ring system. Peaks in the region of 900–700 cm^{-1} are attributed to out-of-plane bending vibrations of aromatic C–H bonds, further confirming the substituted benzene ring structure. Overall, the IR spectral features are consistent with the molecular structure of quercetin, verifying the presence of hydroxyl, carbonyl, and aromatic functional groups and supporting its identification as a polyhydroxylated flavonoid compound.

The Fourier transform infrared (FT-IR) spectrum of kaempferol exhibited characteristic absorption bands consistent with its polyphenolic flavonol structure. A band observed around 3400–3200 cm^{-1} is attributed to stretching vibrations of phenolic O–H groups, indicating the presence of multiple hydroxyl substituents and possible intermolecular hydrogen bonding. bands appearing near 3050–3000 cm^{-1} correspond to aromatic C–H stretching vibrations. spectrum shows absorption band at approximately 1660–1650 cm^{-1}, which is assigned to the conjugated carbonyl (C=O) stretching vibration of the flavonol backbone. The bands in the region of 1600–1500 cm^{-1} are characteristic of aromatic C=C stretching vibrations within the benzene rings of the flavonoid structure. Additional peaks around 1450–1400 cm^{-1} are attributed to C–H bending and phenolic O–H deformation modes. In the fingerprint region, strong absorption bands observed between 1300 and 1000 cm^{-1} correspond to C–O stretching vibrations of phenolic and aryl ether groups, which are typical of flavonoid compounds. Notable peaks around

1270–1210 cm^{-1} and 1170–1050 cm^{-1} are associated with C–O–C and C–O stretching of the pyran and phenolic moieties. The bands appearing in the region of 900–700 cm^{-1} are assigned to out-of-plane bending vibrations of aromatic C–H, confirming the substituted benzene ring system present in kaempferol. the observed absorption bands and their assignments are in good agreement with the expected functional groups of kaempferol, confirming the presence of hydroxyl, conjugated carbonyl, and aromatic structural features typical of this flavonol compound.

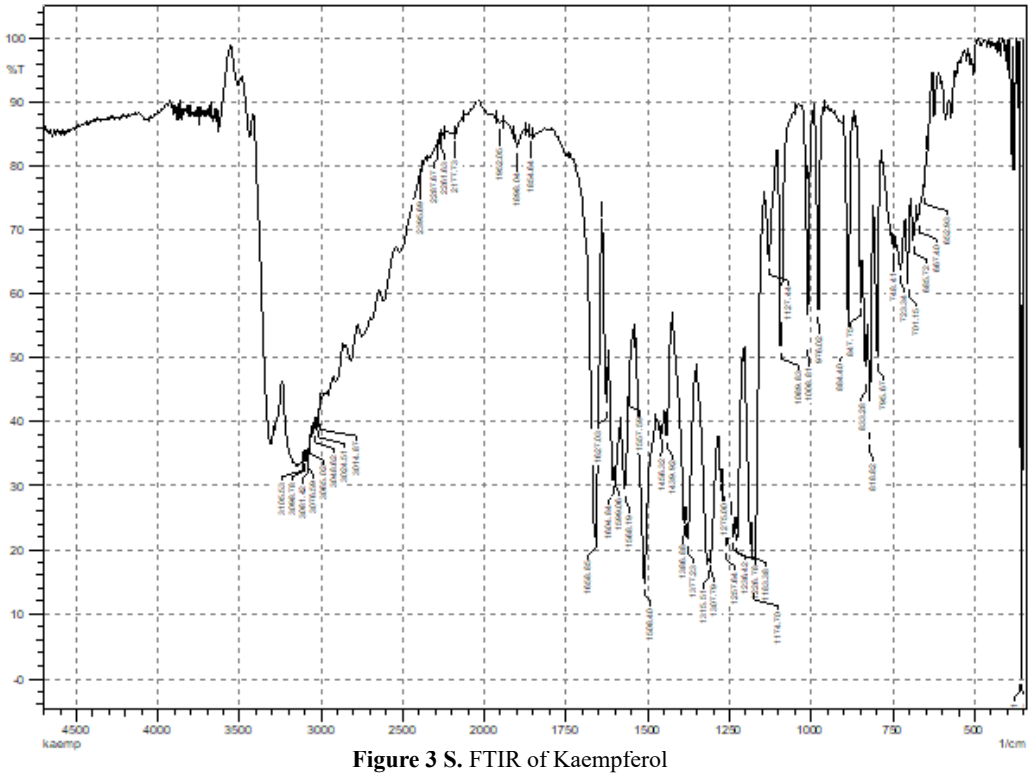

Figure 3 S. FTIR of Kaempferol

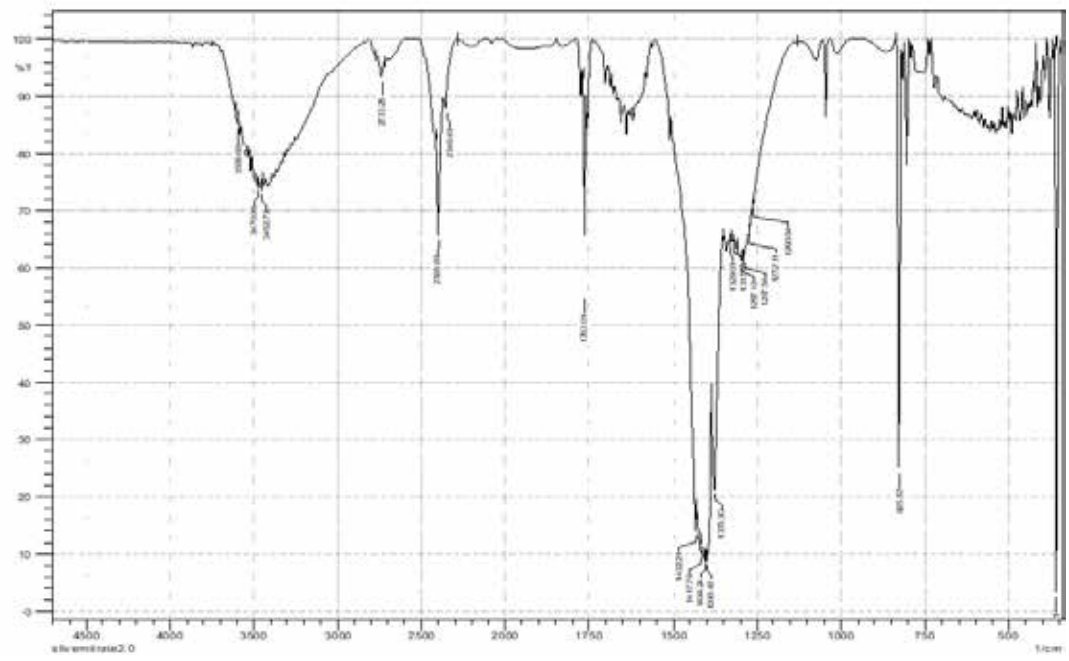

Figure 4 S. FTIR spectra of silver nitrate

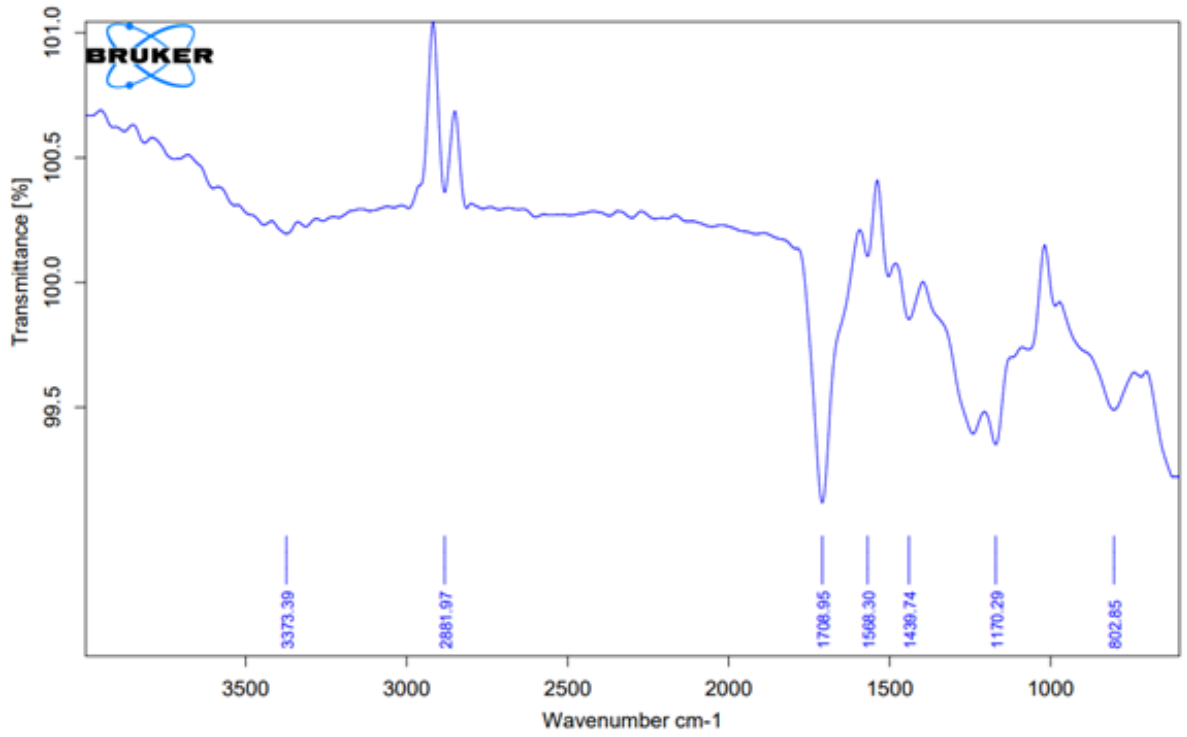

Figure 5 S. FTIR spectra of Carbopol 934

The FT-IR spectrum of silver nitrate displayed characteristic absorption bands corresponding to the nitrate anion and associated functional vibrations. A broad band observed in the region around 3500–3400 cm^{-1} is attributed to O–H stretching vibrations, which are commonly associated with adsorbed moisture or hydrogen-bonded water molecules present in the sample. Weak bands near 2900–2700 cm^{-1} may be assigned to overtone or combination bands, or minor environmental contaminants, as silver nitrate itself does not contain aliphatic C–H bonds. A strong and prominent absorption band observed near 1760–1740 cm^{-1} is associated with the asymmetric stretching vibration of the nitrate (NO_3^-) group, although this band may also be influenced by combination modes. The most intense and characteristic peaks appear in the region between 1500 and 1300 cm^{-1}, corresponding to the asymmetric N–O stretching vibrations of the nitrate ion. In the present spectrum, strong absorptions around 1410–1370 cm^{-1} confirm the presence of the NO_3^- functional group. Additional bands observed between 1300 and 1000 cm^{-1} are attributed to the symmetric stretching vibrations and bending modes of the nitrate group. Peaks in the region of approximately 850–820 cm^{-1} are assigned to out-of-plane bending vibrations of the NO_3^- ion. The absence of organic functional group absorptions and the dominance of nitrate-related bands indicate the purity of the inorganic silver nitrate sample. Overall, the observed absorption pattern is consistent with the characteristic infrared features of silver nitrate, confirming the presence of the nitrate anion coordinated to silver ions.

The FT-IR spectrum of Carbopol 934 exhibited characteristic absorption bands consistent with crosslinked poly (acrylic acid). A broad band observed around 3373 cm^{-1} corresponds to O–H stretching vibrations of carboxylic acid groups involved in extensive hydrogen bonding. The band near 2881 cm^{-1} is attributed to aliphatic C–H stretching of the polymer backbone. A strong absorption at approximately 1708 cm^{-1} represents the carbonyl (C=O) stretching vibration of carboxylic acid functionalities, confirming the presence of polyacrylic acid structure. The band around 1568 cm^{-1} may be associated with asymmetric stretching of carboxylate groups, suggesting partial ionization or intermolecular interactions. Peaks near 1439 cm^{-1} correspond to CH_2 bending and symmetric carboxylate vibrations. Strong absorption around 1170 cm^{-1} is assigned to C–O stretching of carboxylic groups. The band near 802 cm^{-1} corresponds to polymer backbone deformation vibrations. Overall, the observed spectral features are consistent with reported FT-IR characteristics of Carbopol 934.

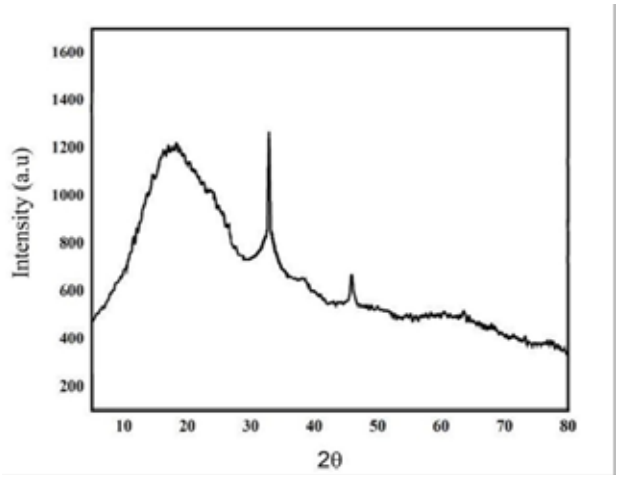

Figure 6 S. XRD crystallogram of prepared KSNPs

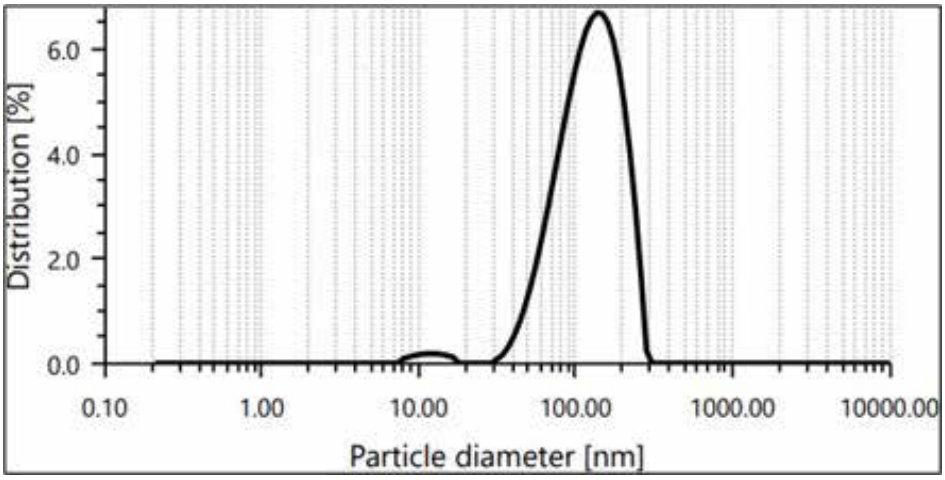

Figure 7 S. Particle size of optimized formulation

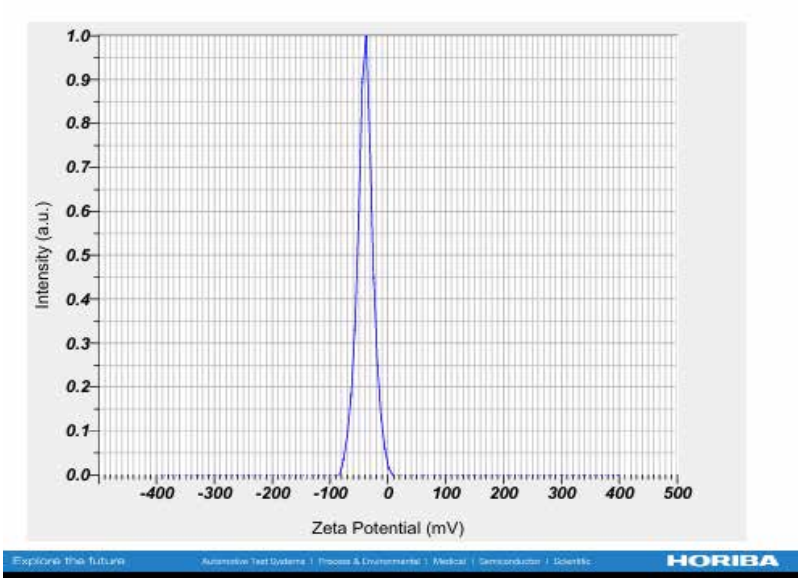

Figure 8 S. Zeta potential of optimized formulation

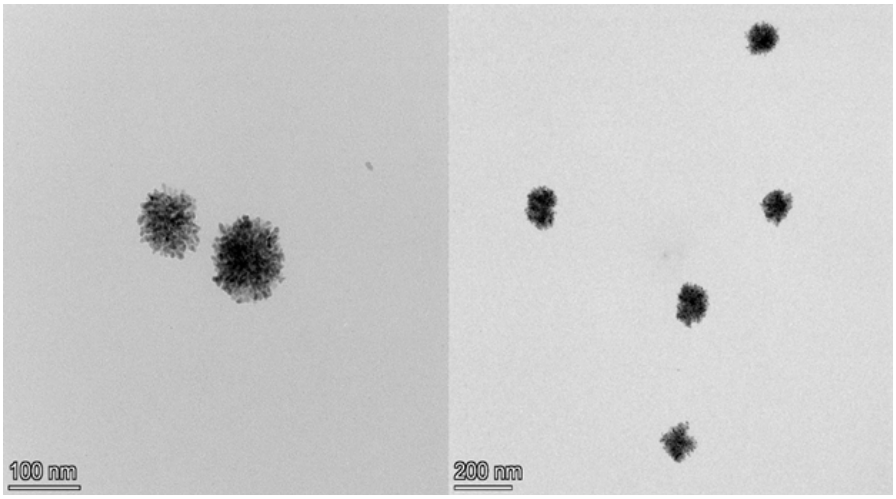

Figure 9 S. Morphology study by TEM analysis of KSNP formulation

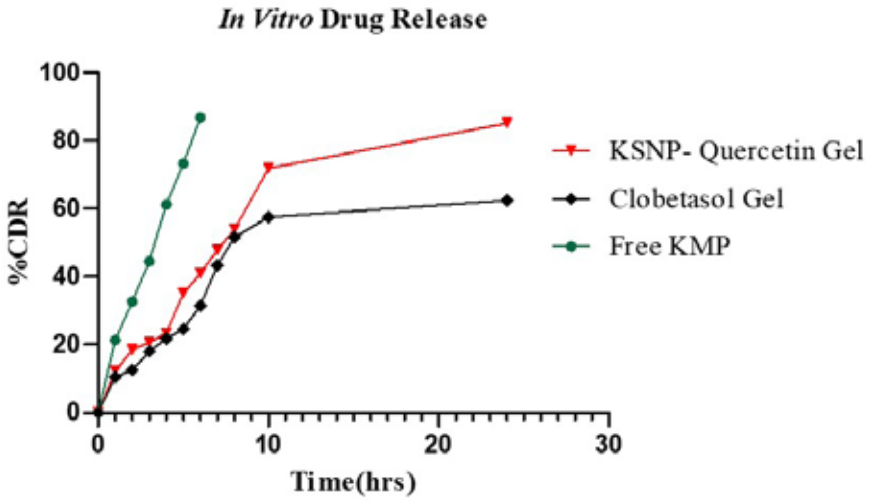

Figure 10 S. Drug release study of KSNP-loaded QRT gel and Marketed preparation of Clobetasone gel

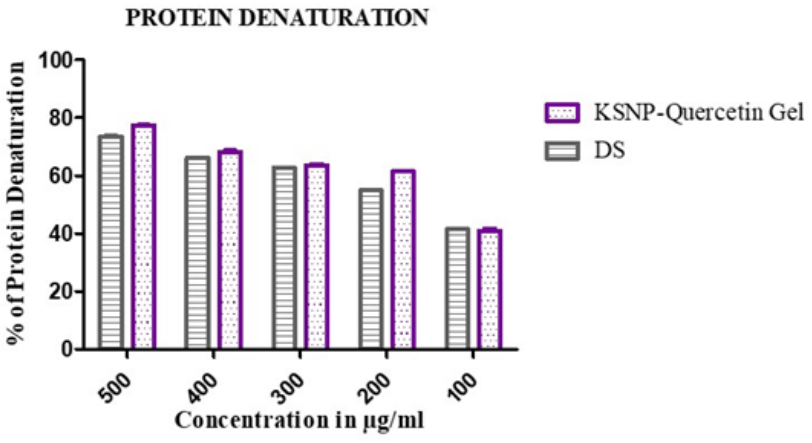

Figure 11 S. *In vitro* anti-inflammatory activity by protein denaturation inhibition method

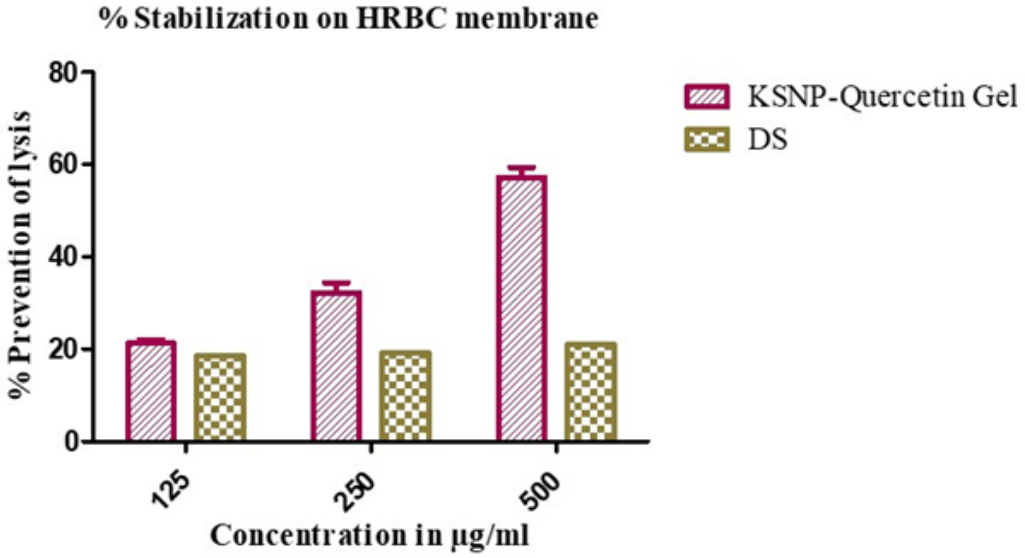

Figure 12 S. *In vitro* anti-inflammatory activity by HRBC membrane stabilization method

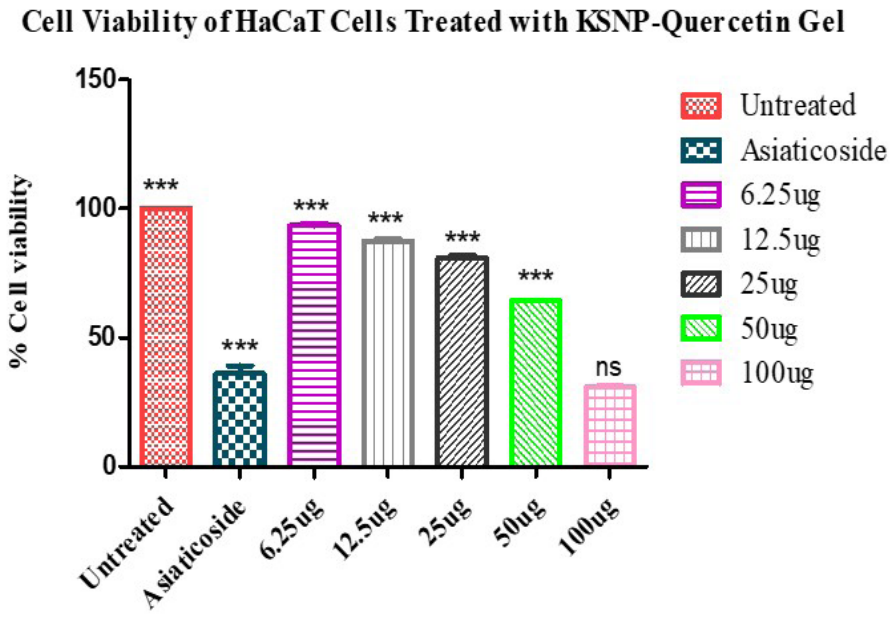

Figure 13 S. *In vitro* anti-psoriatic activity by Sulphorhodamine B assay.

References

[1] Pan R, Zhang J. Epidemiology and treatment of psoriasis: a Chinese perspective. Psoriasis: Targets and Therapy 2014;4:37-47.

[2] Armstrong AW, Blauvelt A, Callis Duffin K, Huang YH, Savage LJ, et al. Psoriasis. Nat Rev Dis Primers 2025;11:1-25.

[3] Psoriasis: assessment and management. London: National Institute for Health and Care Excellence (NICE); 2017 Sep 1. (NICE Clinical Guidelines, No. 153.).

[4] Crisan D, Scharffetter-Kochanek K, Crisan M, Schatz S, Hainzl A, et al. Topical silver and gold nanoparticles complexed with Cornus mas suppress inflammation in human psoriasis plaques by inhibiting NF-κB activity. Exp Dermatol 2018;27:1166-1169.

[5] Carvalho-Silva JM, Reis AC dos. Anti-inflammatory action of silver nanoparticles in vivo: systematic review and meta-analysis. Heliyon 2024;10:34564.

[6] Hussain MS, Altamimi ASA, Afzal M, Almalki WH, Kazmi I,

et al. Kaempferol: Paving the path for advanced treatments in aging-related diseases. Exp Gerontol 2024; 188:112389.
[7] Archoo S, Naikoo SH, Tasduq SA. Role of herbal products as therapeutic agents against ultraviolet radiation-induced skin disorders. Herbal Medicines: A Boon for Healthy Human Life 2022;345-360.
[8] Liu C, Liu H, Lu C, Deng J, Yan Y, et al. Kaempferol attenuates imiquimod-induced psoriatic skin inflammation in a mouse model. Clin Exp Immunol 2019;198:403.
[9] Vollmannová A, Bojňanská T, Musilová J, Lidiková J, Cifrová M. Quercetin as one of the most abundant represented biologically valuable plant components with remarkable chemoprotective effects - A review. Heliyon 2024;10:e33342.
[10] Akhtar J, Badruddeen, Khan MI, Ahmad M, Mishra S. Formulation and optimization of Kaempferol nanoemulsion-based gel for treating skin erythema using Box-Behnken statistical design. Lett Drug Des Discov 2025;22:100132.
[11] Sawant B, Mallya R. Development of quercetin-loaded bilosomes for the management of psoriasis. Current Cosmetic Science. 2025;4:1-10.
[12] Zhang Y, Gong S, Liu L, Shen H, Liu E, et al. Cyclodextrin-coordinated liposome-in-gel for transcutaneous quercetin delivery for psoriasis treatment. ACS Appl Mater Interfaces 2023;15:40228-4040.
[13] Zhu B, Jing M, Yu Q, Ge X, Yuan F, et al. Treatments in psoriasis: from standard pharmacotherapy to nanotechnology therapy. Advances in Dermatology and Allergology/Postępy Dermatologii i Alergologii. 2021;39:460.
[14] Shahriar Ahmed SK, Manchanda Y, De A, Das S, Kumar R. Topical Therapy in Psoriasis. Indian J Dermatol 2023;68:437.
[15] Dogra A, Sachdeva S. Biologic therapy in psoriasis. Indian J Dermatol Venereol Leprol. 2006;72:256.
[16] Strober B, Zhong Y, Sima A, Beeghly A, Eckmann T, et al. Criteria for identifying candidates for systemic psoriasis treatment in the real world: application of the international psoriasis council guidelines in patients in north america. J Psoriasis Psoriatic Arthritis 2024;10:22.
[17] Awlqadr FH, Majeed KR, Altemimi AB, Hassan AM, Qadir SA, et al. Nanotechnology-based herbal medicine: Preparation, synthesis, and applications in food and medicine. J Agric Food Res 2025;19:101661.
[18] Jiang H, Li L, Li Z, Chu X. Metal-based nanoparticles in antibacterial application in biomedical field: Current development and potential mechanisms. Biomed Microdevices 2024;26:12.
[19] Rodrigues AS, Batista JGS, Rodrigues MÁV, Thipe VC, Minarini LAR, et al. Advances in silver nanoparticles: a comprehensive review on their potential as antimicrobial agents and their mechanisms of action elucidated by proteomics. Front Microbiol 2024; 15:1440065.
[20] Xu L, Wang YY, Huang J, Chen CY, Wang ZX, et al. Silver nanoparticles: Synthesis, medical applications and biosafety. Theranostics 2020;10:8996.
[21] Colombo M, de Lima Melchiades G, Michels LR, Figueiró F, Bassani VL, et al. Solid dispersion of kaempferol: formulation development, characterization, and oral bioavailability assessment. AAPS PharmSciTech 2019;20.
[22] Deng SP, Zhang JY, Ma ZW, Wen S, Tan S, et al. Facile synthesis of long-term stable silver nanoparticles by kaempferol and their enhanced antibacterial activity against escherichia coli and staphylococcus aureus. J Inorg Organomet Polym Mater 2021;31:2766-2778.
[23] Ubaid M, Ilyas S, Mir S, Khan AK, Rashid R, et al. Formulation and in vitro evaluation of carbopol 934-based modified clotrimazole gel for topical application. An Acad Bras Cienc 2016;88:2303-2317.
[24] S Rathore RP, Nema RK. Formulation and evaluation of topical gels of carbopol 940. IOSR Journal of Pharmacy and Biological Sciences. 2012;1:70-73.
[25] Jadhav K, Dhamecha D, Bhattacharya D, Patil M. Green and eco-friendly synthesis of silver nanoparticles: Characterization, biocompatibility studies and gel formulation for treatment of infections in burns. J Photochem Photobiol B 2016;155:109-115.
[26] Yadha H, Kolure R, Thakur S, Mandava K, Boddu S. QBD approach for green synthesis of Rutin silver nanoparticles-screening for antioxidant, anticancer, and anticlastogenic potential. Heliyon. 2024;10:e38391.
[27] Patel UD, Mastiholimath VS. Formulation optimization and characterization of bifonazole-loaded transethosomal gel by 32 factorial design for the treatment of topical fungal infection. Bionanoscience 2025;15:1-16.
[28] Angel Morales León J, González Santisteban A, Peña Fuentes D, Guardia Puebla Y, Torres Rodríguez E. In vitro anti-inflammatory activity of aqueous, ethanolic and ethereal extracts of rhizomes, leaves and stems of Anredera vesicaria. J Anal Pharm Res 2018;7.
[29] Kalpana VN, Patra RR, Rajeswari VD. Green synthesis of zinc oxide nanoparticles using fresh stem of cissus quadrangularis extract and its various in vitro studies. Asian J Chem 2017;29:1323-1327.
[30] Vijayalakshmi A, Ravichandiran V, Velraj M, Nirmala S, Jayakumari S. Screening of flavonoid “quercetin” from the rhizome of Smilax china Linn. for anti-psoriatic activity. Asian Pac J Trop Biomed 2012;2:269.
[31] Sampson JH, Raman A, Karlsen G, Navsaria H, Leigh IMMOP. In vitro keratinocyte antiproliferant effect of Centella asiatica extract and triterpenoid saponins. Phytomedicine 2001;8:230-235.
[32] Smajlović A, Haverić A, Alić A, Hadžić M, Smajlović A, et al. Molecular and histopathological profiling of imiquimod-induced dermatosis in Swiss Wistar rats: contribution to the rat model for novel anti-psoriasis treatments. Mol Biol Rep 2021;48:4295-4303.
[33] Singh MP, Chauhan NS, Baldi A. Formulation and Assessment of Topical Gel containing Cassia occidentalis Extract for Anti-Candida Activity. Res J Pharm Technol 2025;18:451-459.
[34] Karbab A, Mokhnache K, Ouhida S, Charef N, Djabi F, et al. Anti-inflammatory, analgesic activity, and toxicity of Pituranthos scoparius stem extract: An ethnopharmacological study in rat and mouse models. J Ethnopharmacol 2020;258.
[35] David L, Moldovan B, Vulcu A, Olenic L, Perde-Schrepler M, et al. Green synthesis, characterization, and anti-inflammatory activity of silver nanoparticles using European black elderberry fruits extract. Colloids Surf B Biointerfaces 2014;122:767-777.
[36] Chen Y, Zhang Q, Liu H, Lu C, Liang CL, et al. Esculetin ameliorates psoriasis-like skin disease in mice by inducing CD4+-Foxp3+ regulatory T cells. Front Immunol 2018;9:410226.
[37] Tian Y, Qi J, Zhang W, Cai Q, Jiang X. Facile, one-pot synthesis, and antibacterial activity of mesoporous silica nanoparticles decorated with well-dispersed silver nanoparticles. ACS Appl Mater Interfaces 2014;6:12038-12045.

[38] Nguyen NPU, Dang NT, Doan L, Nguyen TTH. Synthesis of silver nanoparticles: from conventional to 'modern' methods—a review. Processes 2023;11.
[39] Khalil RM, Abdelbary GA, Basha M, Awad GEA, el-Hashemy HA. Enhancement of lomefloxacin HCl ocular efficacy via niosomal encapsulation: in vitro characterization and in vivo evaluation. J Liposome Res 2017;27:312-323.
[40] Chahardoli A, Hajmomeni P, Ghowsi M, Qalekhani F, Shokoohinia Y, et al. Optimization of quercetin-assisted silver nanoparticles synthesis and evaluation of their hemocompatibility, antioxidant, anti-inflammatory, and antibacterial effects. Global Challenges 2021;5:2100075.
[41] Hooda H, Singh P, Bajpai S. Effect of quercitin impregnated silver nanoparticle on growth of some clinical pathogens. Mater Today Proc 2020;31:625-630.
[42] Mestry M, Rane M, Bajaj A. Commiphora mukul and quercetin loaded liposome gel: potential treatment for psoriasis. Indian Journal Pharm Educ Res 2020;54:654-667.
[43] Gad SC. Alternatives to in vivo studies in toxicology. General, Applied and Systems Toxicology 2011.